

Superconductivity of Alkali Metals under High Pressure

Lei Shi¹ and Dimitrios A. Papaconstantopoulos^{1,2}

¹ *School of Computational Sciences, George Mason University, Fairfax, VA 22030*

² *Center for Computational Materials Science,
Naval Research Laboratory, Washington, DC 20375*

We calculated the superconductivity properties of alkali metals under high pressure using the results of band theory and the rigid-muffin theory of Gaspari and Gyorffy. Our results suggest that at high pressures Lithium, Potassium, Rubidium and Cesium would be superconductors with transition temperatures approaching 10-20 K. Our calculations also suggest that Sodium would not be a superconductor under high pressure even if compressed to less than half of its equilibrium volume. We found that the compression of the lattice strengthens the electron-phonon coupling through a delicately balanced increase of both the electronic and phononic components of this coupling. This increase of the electron-phonon coupling in Li is due to an enhancement of the *s-p* channel of the interaction, while in the heavier elements the *p-d* channel is the dominant component.

I. INTRODUCTION

In the theoretical work of Neaton and Ashcroft¹, a prediction was made that at high pressures Lithium forms a paired ground state. Subsequently, Christensen and Novikov² showed that fcc Lithium under increased pressure may reach a superconducting transition temperature $T_c=50-70$ K. This prediction has been supported by Shimizu et al³ who reported the discovery of superconductivity in compressed Lithium with a $T_c=20$ K. Using a similar methodology, we performed calculations for two other alkali metals, Potassium and Rubidium, and predicted that at high pressures they both would be superconductors with transition temperatures approaching 10 K⁴. Before these works, the only known superconducting alkali metal was Cesium, which becomes superconducting above 7.0 GPa with a transition temperature of about 1.5 K.⁵

In this paper, we have extended our study to Li, Na and Cs using again the theory of electron-phonon interaction in the rigid-muffin-tin approximation (RMTA) formulated by Gaspari and Gyorffy⁶. Our calculations demonstrated that Li and Cs display superconductivity at high pressure above 16 GPa and 3.5 GPa respectively. Our results also showed the lack of superconductivity for Na up to 32 GPa. We compare these new calculations with our previous results of K and Rb to show a complete picture of superconductivity properties of alkali metals under high pressure. Our calculations indicate that the *s-p* channel of contribution to the Hopfield parameter dominates Li under high pressure, while the *p-d* channel contribution is the major reason that K, Rb and Cs become superconductors under high pressure.

Tomita et al⁷ recently reported experimental results for Li, Na and K. They confirmed the superconductivity of Li above 20 GPa at temperatures reaching 15 K. They also pointed out the absence of superconductivity in Na for pressure in the 35-65 GPa range. The contradiction between experiment and

our calculations in K requires further investigation of the plausible phase transitions of K under high pressure which might push it to sufficient pressure for the superconductivity to occur.

II. THEORY

Using the BCS theory, McMillan developed an approach to determine the electron-phonon coupling constant λ and the critical transition temperature T_c for superconductivity.⁸ McMillan's strong coupling theory defines an electron-phonon coupling constant by:

$$\lambda = \frac{\eta}{M \langle \omega^2 \rangle} = \frac{N(\epsilon_F) \langle I^2 \rangle}{M \langle \omega^2 \rangle} \quad (1)$$

where M is the atomic mass; η is the Hopfield parameter⁹ that equals the product of the total density of states, $N(\epsilon_F)$, at the Fermi level, ϵ_F , times $\langle I^2 \rangle$ which is the square of the electron-ion coupling matrix element at ϵ_F averaged over the Brillouin zone; and $\langle \omega^2 \rangle$ is the averaged phonon frequency.

The above theoretical works have provided a way to calculate the transition temperature for superconductivity based on energy band calculations. McMillan proposed the following equation for T_c :

$$T_c = \frac{\langle \omega \rangle}{1.2} \exp\left[\frac{-1.04(1 + \lambda)}{\lambda - \mu^*(1 + 0.62\lambda)}\right] \quad (2)$$

where μ^* is the Coulomb pseudopotential, and $\langle \omega \rangle$ is determined from the Debye temperature Θ_D as follows after converting the units between the ω and the Θ_D :

$$\omega^2 = \frac{1}{2} \Theta_D^2 \quad (3)$$

Gaspari and Gyorffy formulated the RMTA that provides a quantitative tool for determining the

electron-phonon coupling.⁶ This approach has been applied to calculate the parameter η and subsequently T_c . In the RMTA $\langle I^2 \rangle$ is given by

$$\langle I^2 \rangle = \left(\frac{\epsilon_F}{\pi^2} \right) \frac{1}{N^2(\epsilon_F)} \sum_l 2(l+1) \left| \int_0^{R_s} dr r^2 u_l \frac{dv}{dr} u_{l+1} \right|^2 \frac{N_l N_{l+1}}{N_l^{(1)} N_{l+1}^{(1)}} \quad (4)$$

where R_s is the muffin-tin radius, u_l is the radial wave function, $N(\epsilon_F)$ is the total DOS per spin, $N_l(\epsilon_F)$ is the l th component of the density of states, and $N_l^{(1)}$ is a free single scatterer, which is defined as the portion of electrons that is kept inside one single muffin-tin sphere with no other spheres around it and v is the crystal potential. The free scatterer DOS is written as:

$$N_l^{(1)} = \frac{\sqrt{\epsilon_F}}{\pi} (2l+1) \int_0^{R_s} r^2 u_l^2(r, \epsilon_F) dr \quad (5)$$

Gaspari and Gyorffy found that the matrix elements in Eq. 4 can be evaluated exactly:

$$\left| \int_0^R dr r^2 u_l \left(\frac{dv}{dr} \right) u_{l+1} \right|^2 = \sin^2(\delta_{l+1} - \delta_l) \quad (6)$$

where δ_l are scattering phase shifts given in terms of the logarithmic derivative of the radial function¹⁰ L_l :

$$L_l = \frac{u'_l(R_s, \epsilon_F)}{u_l(R_s, \epsilon_F)} = \frac{\cos(\delta_l(\epsilon_F)) j'_l(kR_s) - \sin(\delta_l(\epsilon_F)) n'_l(kR_s)}{\cos(\delta_l(\epsilon_F)) j_l(kR_s) - \sin(\delta_l(\epsilon_F)) n_l(kR_s)} \quad (7)$$

so that:

$$\tan \delta_l(R_s, \epsilon_F) = \frac{j'_l(kR_s) - j_l(kR_s) L_l(R_s, \epsilon_F)}{n'_l(kR_s) - n_l(kR_s) L_l(R_s, \epsilon_F)} \quad (8)$$

where, l indicates the angular momentum; j_l is the spherical Bessel function; n_l is the spherical Neumann function; u_l is the usual scattering solution of the radial Schrödinger equation; $k = \sqrt{\epsilon_F}$, and R_s is the muffin-tin radius.

Then, $\langle I^2 \rangle$ is written as:

$$\langle I^2 \rangle = \frac{\epsilon_F}{\pi^2} \sum_l 2(l+1) \frac{\sin^2(\delta_{l+1} - \delta_l)}{N_l^{(1)} N_{l+1}^{(1)}} \frac{N_l N_{l+1}}{N^2(\epsilon_F)} \quad (9)$$

We have moved $N(\epsilon_F)$ inside the sum in the spirit of Pickett's¹¹ reinterpretation of the RMTA. This allows us to isolate the ratio of $N_l(\epsilon_F)/N(\epsilon_F)$, which will play an essential role in the explanation of the alkali metals being superconducting under high pressure.

III. COMPUTATIONAL PROCEDURE

We applied the theory discussed above to calculate the superconducting transition temperatures of alkali metals under high pressure. The computational procedure is shown in Fig. 1. We first performed Augmented PlaneWave (APW) calculations of the band structures and total energies of the targeted alkali metals in the local density approximation(LDA) following the Hedin-Lundqvist prescription¹² in both *bcc* and *fcc* structures, for a wide range of volumes reaching high pressures. From these calculations we obtained the Fermi level ϵ_F , values of the total density of states $N(\epsilon_F)$ and their angular momentum decompositions $N_l(\epsilon_F)$ as a function of volume. We also used the APW results to determine the volume variation of the bulk moduli B . We then used the self-consistent APW potentials to determine the scattering phase shift $\delta_l(R_s, \epsilon_F)$ again as a function of volume. The quantities N_l and δ_l were then used in the RMTA to determine the Hopfield parameter η . The next step was to calculate the electron-phonon interaction parameter by Eq. 1. We have accomplished this by assuming that¹³

$$\langle \omega^2 \rangle = CB(V) V^{1/3} \quad (10)$$

We determined the constant of proportionality C from the experimental value of the bulk modulus B , the volume V , and the Debye temperature Θ_D using Eq. 3. Finally, we estimated the transition temperature T_c using Eq. 2, setting the Coulomb pseudopotential $\mu^* = 0.13$.

IV. RESULTS

To demonstrate the effect of high pressures on the band structure of alkali metals in Fig. 2 we plotted the bands of *bcc* Cs at the lattice parameters of 10.8 *a.u.* and 8.8 *a.u.* that correspond to 0 and 4.8 GPa pressures respectively. Fig. 2 demonstrates a significant increase of the *d*-band width $H_{25'}-H_{12}$, from a value of 0.34 *Ry* at zero pressure to 0.59 *Ry* at 4.8 GPa. In Fig. 3, we note a marked increase of the *d*-like density of states $N_d(\epsilon_F)$ under high pressure. We also note in the plot of the band structure that the state H_{12} , which has pure *d* character, is above ϵ_F at normal lattice constant and below in the compressed lattice. This causes the increase of $N_d(\epsilon_F)$, which is shown in the DOS graph. This increase of the *d* density of states makes the largest contribution to the large value of η at small volumes as discussed below. We also observed this trend for compressed *fcc* Cs and for the other alkali metals K and Rb. In contrast, for both the *bcc* and *fcc* phases of Li and Na, the density of states decreases as the lattice is compressed. This fact gives a partial explanation of

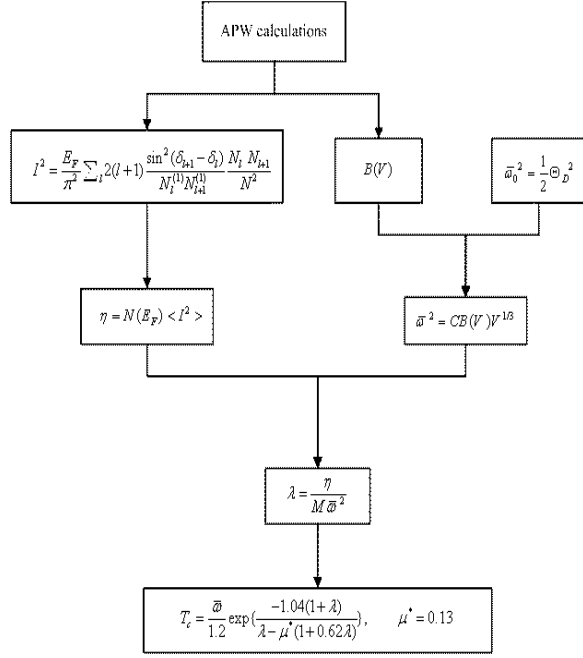


FIG. 1: The procedure of calculating the transition temperature T_c .

the absence of superconductivity under high pressure for Na. For Li, however, the increase in the matrix elements $\langle I^2 \rangle$ is strong enough to ensure the overall large increase in η , which we will discuss later.

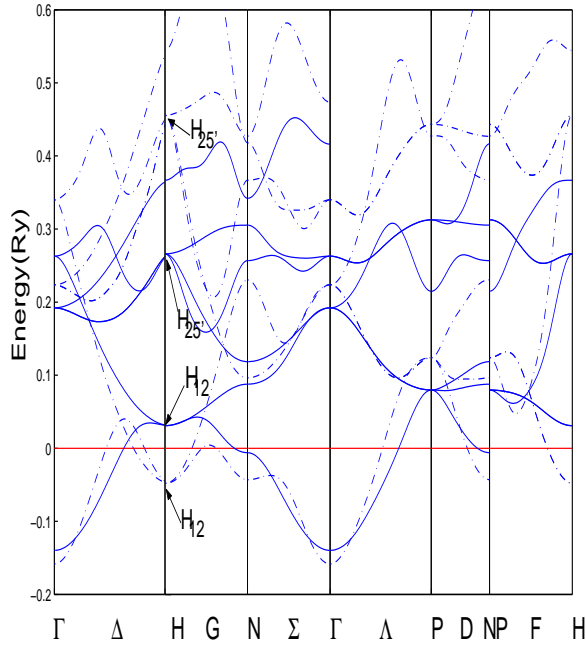


FIG. 2: Band structure of *bcc* Cs, the solid and dashed lines represent the lattice parameter $a=10.8a.u.$ and $a=8.8a.u.$ respectively.

From the band calculations, we obtained the ϵ_F , the total density of states $N(\epsilon_F)$, and their angular

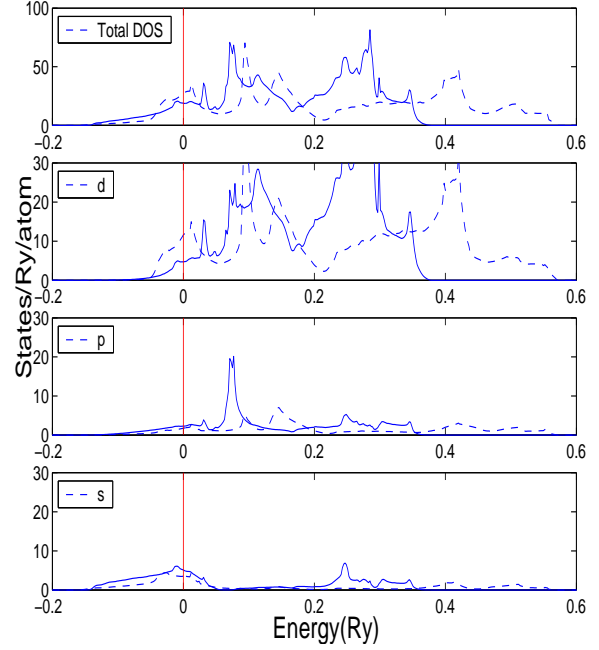


FIG. 3: Density of states of *bcc* Cs, the solid and dashed lines represent the lattice parameter $a=10.8a.u.$ and $a=8.8a.u.$ respectively.

momentum decompositions N_l as a function of volume. We show the ratios $N_l(\epsilon_F)/N(\epsilon_F)$ as a function of volume in Fig. 4. These ratios are crucial in the determination of η . It is important to note that the ratio $N_d(\epsilon_F)/N(\epsilon_F)$ of the heavier alkali metals K, Rb and Cs increases rapidly as a function of decreasing volume. The buildup of the *d*-like DOS under high pressure causes the large values of η at small volumes shown in Fig. 4. Our results for Cs generally agree with previous experiments and theoretical calculations of the *s-d* electronic transition under high pressure.^{14,15,16} For Li and Na, the *p* and *d* components of the density of states remain almost constant while the *s* component decreases slowly with increasing pressure. This causes the decrease of the total density of states of Li and Na. Our Li DOS results also agree with the Christensen and Novikov calculations.²

We then used the self-consistent APW potentials to determine the scattering phase shift δ_l and the free scatterers $N_l^{(1)}$, again using Eq. 5 discussed in section II as a function of volume, to determine the Hopfield parameter η .

As an example, we show the phase shifts of Rubidium in the *bcc* structure in Fig. 5. The left and right panels of the graph show the phase shift of the *s*, *p*, *d*, and *f* states under normal and high pressure respectively. In this graph, we see that the difference of the phase shift $\delta_d - \delta_p$ increases dramatically when the lattice is compressed, while the difference of the phase shift $\delta_p - \delta_s$ reduces by a small amount. Since the function $\sin(x)$ monotonically increases in

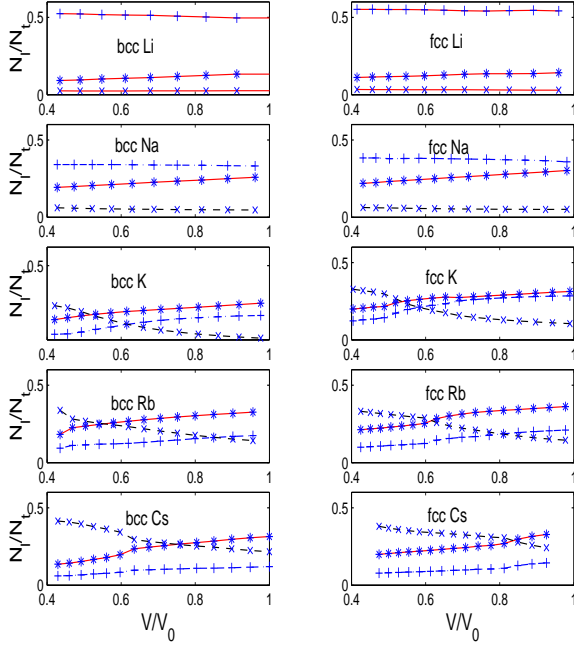


FIG. 4: Angular momentum decomposed DOS divided by the total DOS at ϵ_F . The symbol * denotes s, the symbol + denotes p and the symbol x denotes d states.

the range $[0, \frac{\pi}{2}]$, the large increase of $\delta_d - \delta_p$ results in the large increase of the term $\sin^2(\delta_d - \delta_p)$ and, hence, $\langle I^2 \rangle$ referring to Eq. 9.

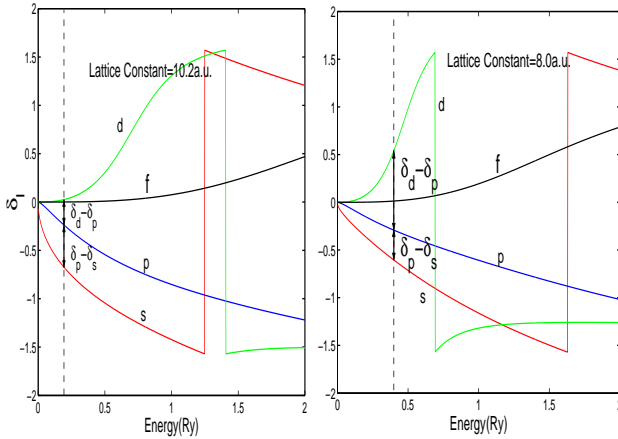


FIG. 5: Phase shift of bcc Rb under normal and high pressure.

Fig. 6 shows that η in all five alkali metals in the bcc and fcc lattices increases significantly and in the same manner with decreasing volume. Among all alkali metals, Li has the largest increase of η with decreasing volume, which is one of the reasons why Li is a superconductor under high pressure.

In Fig. 7, we show the η contributions from s - p , p - d and d - f scattering channels as a function of volume in both the bcc and fcc structures. This graph shows that different elements have different scatter-

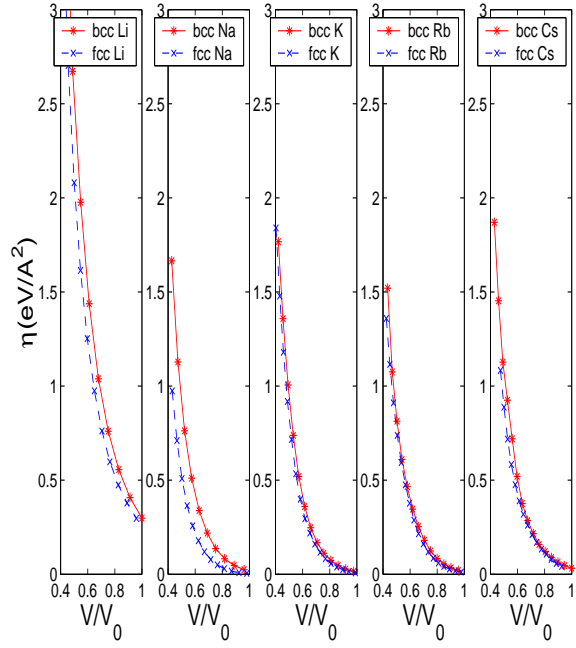


FIG. 6: Hopfield parameter η as a function of volume.

ing channels as the dominant contributors to the total η . More specifically for Li and Na, the η contribution of the s - p channel increases rapidly with compressing volume while the other two contributions stay around zero. For K and Rb, when volume is compressed the η contributions from both the s - p and p - d channels increase quickly. For Cs, the p - d channel contributes the major increase of η with volume compression. For all elements, the η contribution of d - f channel is always very close to zero. The graph demonstrates that the largest portion of the η increase in Li under high pressure is contributed by the s - p channel. Na shows a small increase of η compared to Li that is generated by the s - p channel.

Fig. 8 illustrates the volume variation of the electron-ion coupling matrix element $\langle I^2 \rangle$. In particular, we should note that the $\langle I^2 \rangle$ of Li increases significantly with decreasing volume. In fact it is about two times larger than in the other four alkali metals. This explains the increase of η in Li with decreasing volume despite the decrease of $N(\epsilon_F)$.

The next step was to calculate the average phonon frequency $\langle \omega \rangle$. We have accomplished this by assuming that it is proportional to the product of the bulk modulus B and the cubic root of the volume (see Eq. 10). We determined the constant of proportionality C from the experimental values of B , V and the Debye temperature Θ_D under ambient pressure using Eqs. 3 and 10 and we obtained:

$$C = \frac{\frac{1}{2}\Theta_D^2}{B(V_0)V_0^{\frac{1}{3}}} \quad (11)$$

Fig. 9 shows the increase of the bulk modulus

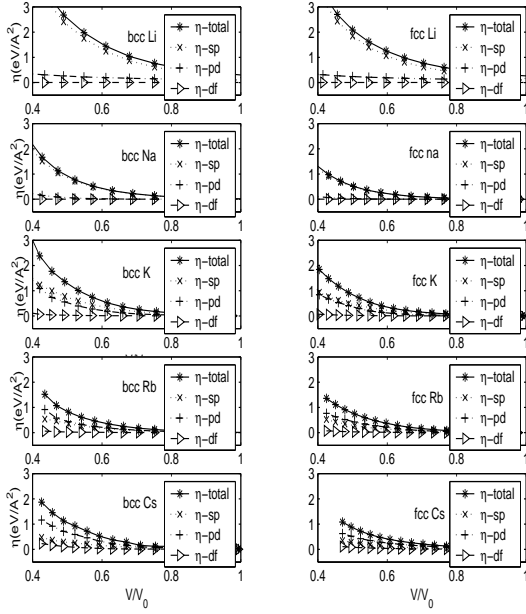


FIG. 7: Total η and its contributions from the s - p , p - d and d - f channels.

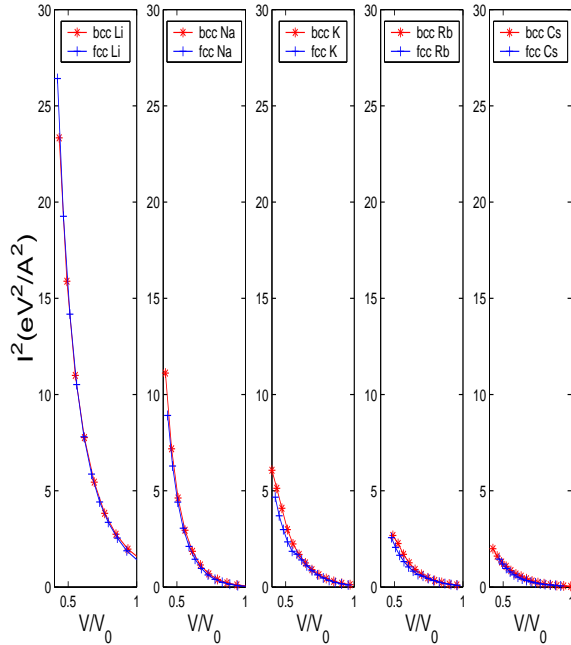


FIG. 8: Electron-ion coupling matrix elements $\langle I^2 \rangle$ as a function of volume.

B and force constant $M\langle\omega^2\rangle$ as a function of decreasing volume. In this plot, we note that the bulk moduli of Li and Na increase dramatically with lattice compression. The bulk modulus increase of K, Rb and Cs is around 1/3 of the amount for Li and Na.

Combining the values of the Hopfield parameters and the averaged phonon frequency, we determined

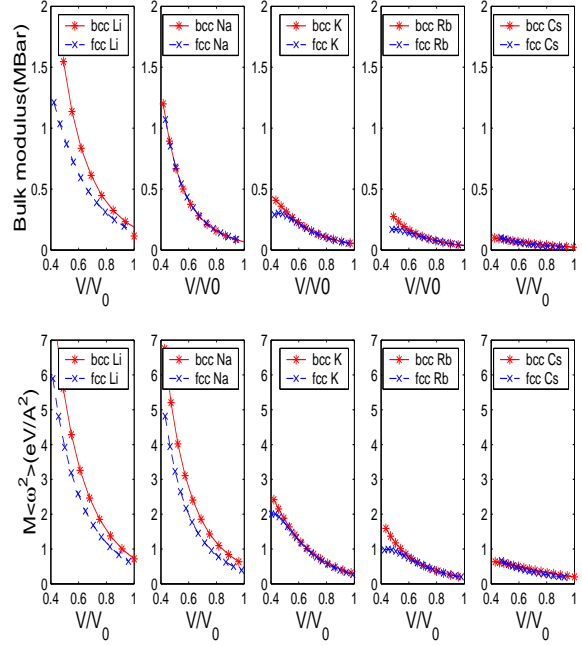


FIG. 9: The bulk moduli B and force constants $M\langle\omega^2\rangle$ as a function of volume.

the electron-phonon coupling constant using Eq. 1. In Fig. 10, we show the electron-phonon coupling constant λ as a function of volume. It is evident that for the alkali metals Li, K, Rb, and Cs, at small volumes, λ reaches large values suggesting that these metals could display superconductivity under pressure. To quantify our predictions for superconductivity on the basis of strong electron-phonon coupling, we have calculated T_c for all five elements in both the bcc and fcc structures at high pressure using Eq. 2 with a Coulomb pseudopotential value $\mu^* = 0.13$.

Table I summarizes our results for $N(E_F)$, $\langle I^2 \rangle$, η , λ , $M\langle\omega^2\rangle$, $\langle\omega\rangle$ and T_c of the five alkali metals in both bcc and fcc structures under high and zero pressure.

Fig. 11 shows the prefactor, averaged phonon frequency, $\langle\omega\rangle$ in the Mcmillan equation. We note in this graph that the $\langle\omega\rangle$ for Li, in both bcc and fcc structures, increases much faster than in the other alkali metals under high pressure. This is the other reason that Li has larger T_c than those of K, Rb, and Cs despite the fact that the λ of K, Rb, and Cs can be larger than that of Li under high pressure.

Fig. 12 shows the transition temperature T_c of the five alkali metals in both bcc and fcc structures as a function of volume. As one might expect from the large values of the electron-phonon interaction λ , the elements Li, K, Rb, and Cs are predicted to be superconductors under high pressures that correspond to 16, 10, 8.9, and 3.5 GPa respectively.

Our calculations suggest that Na does not display superconductivity because the electron-phonon coupling constant λ remains small ($\lambda \approx 0.25$) for com-

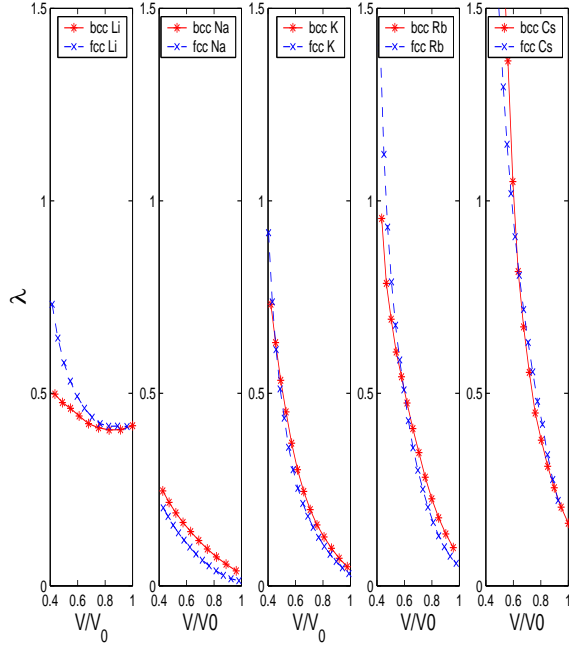


FIG. 10: Electron-phonon coupling constant λ as a function of volume.

TABLE I: $N(E_F)$ (States/eV/atom), I^2 (eV²/Å²), η (eV/Å²), $M\langle\omega^2\rangle$ (eV/Å²), λ , ω (K) and T_c (K) at ambient and high pressure.

| | | lat. | $N(E_F)$ | I^2 | η | $M\omega^2$ | λ | ω | T_c |
|----|-----|------|----------|-------|--------|-------------|-----------|----------|-------|
| Li | bcc | 5.0 | 0.23 | 15.9 | 3.65 | 7.34 | 0.50 | 658.8 | 16.5 |
| | | 6.6 | 0.29 | 1.11 | 0.30 | 0.71 | 0.42 | 243.9 | 0.52 |
| | | 6.0 | 0.18 | 26.7 | 4.67 | 5.90 | 0.73 | 627.7 | 18.8 |
| | | 8.0 | 0.27 | 1.41 | 0.38 | 0.64 | 0.41 | 241.8 | 0.6 |
| Na | bcc | 5.8 | 0.15 | 11.1 | 1.67 | 6.75 | 0.25 | 407.2 | 0.0 |
| | | 7.6 | 0.23 | 0.11 | 0.03 | 0.63 | 0.04 | 124.7 | 0.0 |
| | | 7.4 | 0.15 | 8.87 | 1.33 | 4.81 | 0.20 | 343.9 | 0.0 |
| | | 9.6 | 0.22 | 0.08 | 0.02 | 0.50 | 0.02 | 110.5 | 0.0 |
| K | bcc | 7.4 | 0.43 | 4.10 | 1.77 | 2.42 | 0.73 | 186.8 | 5.6 |
| | | 9.8 | 0.40 | 0.04 | 0.02 | 0.31 | 0.05 | 67.1 | 0.0 |
| | | 9.2 | 0.50 | 3.72 | 1.84 | 2.00 | 0.91 | 170.2 | 8.7 |
| | | 11.8 | 0.35 | 0.11 | 0.04 | 0.47 | 0.08 | 82.5 | 0.0 |
| Rb | bcc | 8.0 | 0.57 | 2.67 | 1.51 | 1.59 | 0.95 | 102.6 | 5.6 |
| | | 10.4 | 0.51 | 0.04 | 0.02 | 0.21 | 0.10 | 37.0 | 0.0 |
| | | 10.0 | 0.53 | 2.57 | 1.36 | 0.97 | 1.40 | 80.2 | 7.7 |
| | | 13.2 | 0.47 | 0.03 | 0.02 | 0.20 | 0.06 | 36.3 | 0.0 |
| Cs | bcc | 8.6 | 0.94 | 1.99 | 1.87 | 0.63 | 2.95 | 51.9 | 8.8 |
| | | 11.2 | 0.77 | 0.06 | 0.05 | 0.23 | 0.20 | 30.9 | 0.0 |
| | | 11.2 | 0.75 | 1.45 | 1.08 | 0.67 | 1.63 | 53.1 | 6.0 |
| | | 14.0 | 0.67 | 0.06 | 0.04 | 0.19 | 0.22 | 28.3 | 0.0 |

pressions up to 32 GPa as shown in Fig. 10. There are three factors determining that λ of Na under high pressure is not large enough to become a superconductor: (1)decreasing density of states at the Fermi level with volume compression, which is also the case for Li; (2)Na does not have large $\langle I^2 \rangle$ like Li un-

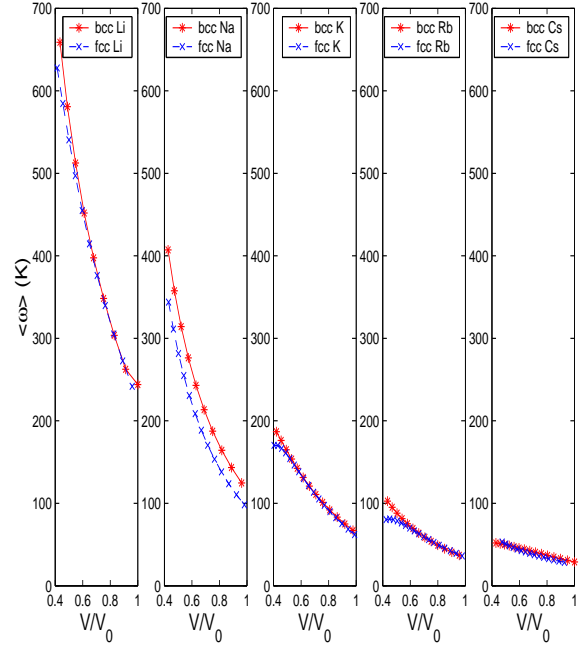


FIG. 11: Averaged phonon frequency $\langle\omega\rangle$ as a function of volume.

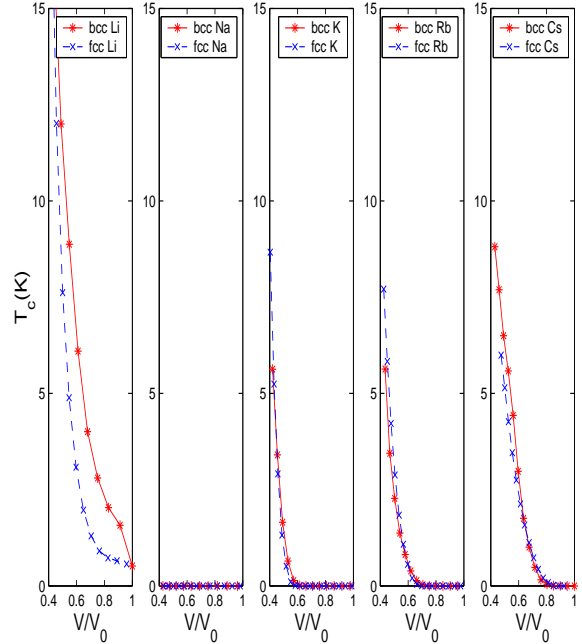


FIG. 12: Transition temperature T_c as a function of volume.

der high pressure; and (3)the bulk modulus of Na increases more rapidly than in the heavier alkali metals K, Rb and Cs, which results in a large force constant $M\langle\omega^2\rangle$. More detailed results from these calculations can be found in Ref.¹⁷.

V. CONCLUSIONS

According to the McMillan equation, the electron-phonon coupling constant λ is the essential parameter in the determination of the transition temperature T_c . Increase of λ under high pressure results in the increase of T_c . λ is calculated by the ratio of the Hopfield parameter η and force constant $M\langle\omega^2\rangle$. The increase of λ with decreasing volume is caused by either an increase of η or a decrease of $M\langle\omega^2\rangle$, or appropriate combinations of these two factors. For K, Rb, and Cs, because the increase of the bulk modulus under pressure is slow, the increase of η , which is mainly caused by an increase of $N(\epsilon_F)$, will dominate the determination of λ . Therefore, K, Rb, and Cs have a large λ under high pressure, which results in the prediction of superconductivity. The large increase of η in Li under high pressure is due to the quick increase of $\langle I^2 \rangle$ and the rapid increase of the prefactor $\langle\omega\rangle$, which dominate at small volume, instead of $N(\epsilon_F)$, which is actually decreasing. Thus, Li still has a large λ under high pressure although its $N(\epsilon_F)$ decreases and the bulk modulus increases with volume compression. Therefore, Li would be a superconductor under high pressure. Na is different from Li and from the other alkali metals because Na has a decreasing $N(\epsilon_F)$ and also a fast increasing bulk

modulus under pressure. In addition, the $\langle I^2 \rangle$ of Na is not increasing quickly enough to ensure large η under high pressure. This is basically the reason why our calculations suggest the absence of superconductivity for Na under high pressure.

The similarity of our *fcc* and *bcc* results suggests that our prediction of superconductivity in K, Rb, and Cs appears to be nearly independent of crystal structure. We believe that our predictions are still valid even if, experimentally, these materials under high pressure transform to other structures such as *hR1* or *cI16*. We suggest that the mechanism of superconductivity in K, Rb, and Cs is due to the increased *d*-like character of the wave functions at ϵ_F at high pressures, which validates our use of the RMTA that is successful in transition metals as shown by Papaconstantopoulos et al.¹⁸ It should also be mentioned that we performed GGA calculations on these materials and our final results are nearly independent of the form of exchange and correlation used. Clearly our results for the value of T_c are sensitive to the value of μ^* , which was fixed to the common value of 0.13 in this work.

Acknowledgment: We wish to thank Dr. Michael J. Mehl for valuable discussions and comments and the US Office of Naval Research for partial support.

-
- ¹ J.B. Neaton and N.W. Ashcroft, *Nature*, 400, 141 (1999)
 - ² N.E. Christensen and D.L. Novikov, *Phys. Rev. Lett.* 86, 1861 (2001)
 - ³ K. Shimizu, H. Ishikawa, D. Takao, T. Yagi and K. Amaya, *Nature*, 419, 597-599 (2002).
 - ⁴ Lei Shi, D. A. Papaconstantopoulos, M. J. Mehl, *Solid State Communications*, 127,13-15 (2003)
 - ⁵ Jörg Wittig, *Phys. Rev. Lett.*, 24,812-815 (1970)
 - ⁶ G.D.Gaspari and B.L.Gyorffy, *Phys. Rev. Lett.* 28, 801 (1972);
 - ⁷ Tomita T, Deemyad S, Hamlin JJ, Schilling JS, Tissen VG, Veal BW, Chen L, Claus H, *J. of Phys.- Cond. Mat.* 17 (11): S921-S928 Sp. Iss. SI, MAR 23 2005
 - ⁸ W.L. McMillan, *Phys. Rev.* 167, 331 (1968); P.B. Allen and R.C. Dynes, *Phys. Rev. B* 12, 905 (1975)
 - ⁹ J. J. Hopfield *Phys. Rev.* 186, 443 (1969)
 - ¹⁰ J. M. Ziman *Principles of the theory of solids* Cambridge University Press (1964);
 - ¹¹ Warren E. Pickett, *Phys. Rev. B*, 25,745-754 (1981)
 - ¹² L. Hedin and B. L. Lundqvist. *J. Phys. C:Solid State Phys.* V.4 (1971).
 - ¹³ T. Jarlborg, *Phys. Scr.* 37, 795 (1988)
 - ¹⁴ R. Sternheimer, *Phys. Rev.* 78, 235 (1950)
 - ¹⁵ S. G. Louie and M. L. Cohen, *Phys. Rev. B* 10, 3237 (1974)
 - ¹⁶ D. B. McWhan, G. Parisot and D. Bloch, *J. Phys. F: Metal Phys.* 4, L69 (1974)
 - ¹⁷ Lei Shi, *Electronic Structure Calculations of Materials: Methods and Applications*, Ph.D. Thesis, George Mason University, 2005
 - ¹⁸ D.A. Papaconstantopoulos, L.L. Boyer, B.M. Klein, A.R. Williams, V.L. Moruzzi and J.F. Janak *Phys. Rev. B* 15, 4221 (1977)